33rd Annual International Conference of the IEEE EMBS
Boston, Massachusetts USA, August 30 - September 3, 2011

A Framework for the Online Analysis of Multi-Electrode Gastric Slow Wave Recordings

Simon H. Bull, Greg O'Grady, Leo K. Cheng, Andrew J. Pullan

Abstract— **High resolution mapping of electrical activity is becoming an important technique for analysing normal and dysrhythmic gastrointestinal (GI) slow wave activity. Several methods are used to extract meaningful information from the large quantities of data obtained, however, at present these methods can only be used offline. Thus, all analysis currently performed is retrospective and done after the recordings have finished. Limited information about the quality or characteristics of the data is therefore known while the experiments take place. Building on these offline analysis methods, an online implementation has been developed that identifies and displays slow wave activations working alongside an existing recording system. This online system was developed by adapting existing and novel signal processing techniques and linking these to a new user interface to present the extracted information. The system was tested using high resolution porcine data, and will be applied in future high resolution mapping studies allowing researchers to respond in real time to experimental observations.**

I. Introduction

There is an underlying bioelectrical slow wave activity that has an important role in the coordination of gastrointestinal (GI) contractions, and several motility disorders have been linked to dysrhythmic slow wave behaviour. High resolution multi-electrode mapping is an established technique for characterising this slow wave behaviour and provides insights into the role of electrical activity in health and disease [1], [2].

Current analysis of high resolution GI recordings is performed offline, after recordings are completed. Analysis requires marking the activation times of each slow wave on each electrode. The few online analysis systems that currently exist are unable to provide the spatio-temporal detail that high resolution studies are capable of [3]. However, being restricted to offline analysis imposes several important limitations. Simple issues such as poor electrode contact can unknowingly compromise a study, and an online system would allow such issues to be corrected while mapping.

An online system could also facilitate the monitoring of activity as it occurs by identifying slow wave events as the recordings are being taken. For instance, it may become apparent from the slow wave activity detected and displayed that the electrode platform is not optimally placed over the area of interest, and with that information the electrodes could be moved as required. An online system would enable dynamic experiments such as trials of targeted interventions in response to specific dysrhythmias. Online systems are now widely used in cardiac electrical mapping and this includes the mapping and clinical management of cardiac arrhythmias (Ensite System, St. Jude Medical, Inc., MN, USA).

Manuscript received March 25, 2011. This project and/or authors are supported by funding through the Health Research Council (New Zealand) and National Institute of Health (RO1 DK 64775)

S.H. Bull is with the Auckland Bioengineering Institute, The University of Auckland, New Zealand. Email: s.bull@auckland.ac.nz

G. O'Grady is with the Department of Surgery & the Auckland Bioengineering Institute, The University of Auckland, New Zealand.

L.K. Cheng is with the Auckland Bioengineering Institute, The University of Auckland, New Zealand.

A.J. Pullan is with the Department of Engineering Science & Auckland Bioengineering Institute, The University of Auckland, New Zealand; The Riddet Institute, New Zealand; Department of Surgery, Vanderbilt University, Nashville, TN, USA.

II. Implementation

Existing recording in our laboratory is performed with a Biosemi system and the associated ActiView recording software (Biosemi, Amsterdam, The Netherlands), recording up to 256 channels in a high-resolution (HR) array using unipolar electrodes [4]. This software has a TCP server feature that allows clients to connect to it while running and be streamed the raw data through a socket. Using this feature, a separate program running either on the same machine or a separate machine that is on the same network can receive data at the same time as it is being recorded, without disrupting the recording. The feature was used to create a Python program that receives and decodes the raw data and then processes it using appropriate detection methods to identify recording problems and identify slow wave events, and presents this information to the user.

The concise but informative presentation of information to the user is critical to the success of the online system. HR mapping provides detailed spatio-temporal information but in an online system the user must interpret any provided information at the same rate it is being recorded. Computer animations were chosen as the primary method for communicating with the user, as they are able to convey large quantities of information while being insensitive to noise as the user readily filters isolated noise visually [5].

A. Slow wave detection

Detecting slow waves requires the identification of activation times in each electrode independently. The falling edge variable threshold (FEVT) algorithm [6] has been used to effectively identify large numbers of gastric slow waves offline, after recordings have been taken. Due to its high positive predictive value and low number of false positives, this method was chosen to be implemented in an online context to detect slow wave events as they are being recorded.

There are four aspects to the FEVT method that were implemented: the downsampling and filtering of the raw

signal, the calculation of a transform that accentuates slow waves events, the calculation of a threshold and the selection of points that are slow waves.

1) Filtering: The signals were recorded at a frequency of 512 Hz and received slightly after they were recorded. These were downsampled to 32 Hz for consistency with the FEVT method and to reduce the quantity of data being processed, such that for every 16th received sample the downsampler yields a new value (for each channel). These downsampled values were then filtered using a lowpass butterworth filter with a passband edge frequency of 0.5 Hz and a stopband edge frequency of 4 Hz, as the target signals are in a range below this frequency.

An estimate of the baseline for each signal was removed using a high pass filter with an edge frequency of 1/60 Hz to remove the slow baseline wander [6].

2) Detection Signal: As described by Erickson [6] the downsampled and filtered signals $\{V_i : i \in \mathbb{N}\}$ have a non-linear energy operator (NEO) [7] transformation applied to them (1).

$$\mathrm{NEO}(V_i) = V_i V_i - V_{i-1} V_{i+1} \tag{1}$$

This was then smoothed with a moving average filter with width of one second, or 32 samples at 32 Hz to give a smoothed transform, referred to as the SNEO signal S_t.

The incoming signals were also convolved with an edge detect kernel that gave a positive response when the input signal dropped, and is referred to as E_t. The detection signal was then calculated as the element-wise product of S_t and E_t where that product is positive and zero where it is negative (2).

$$F_t = \begin{cases} S_t E_t & \text{if } S_t E_t \geq 0 \\ 0 & \text{if} S_T E_t < 0 \end{cases} \tag{2}$$

This resulted in a detection signal that is in practice commonly zero, as $S_t E_t$ was less than zero a large proportion of the time, and is equal to or very close to zero more than half of the time as the typical example in Fig. 1 shows.

3) Variable Threshold: The variable threshold was calculated from the detection as a type of median absolute deviation (3).

$$\mathrm{MAD}(X) = \mathrm{median}_i(|X_i - \mathrm{mean}_j(X_j)|) \tag{3}$$

The threshold at a particular point in time is calculated as the median absolute deviation of the detection signal in a window surrounding that point in time, multiplied by a tunable scalar parameter. The width of the window that was found to be most effective was 30 seconds (15 seconds forward and 15 backward), or 960 samples at 32 Hz. The most effective scalar multiplier was 5.9 [6]. Using the definition for the median absolute deviation described in (3) took a large amount of processing time, as the absolute operator meant that it was not possible to simply retain a sorted structure and update it at each step.

However, it was observed that in the majority of channels the detection signal was either zero or very close to zero

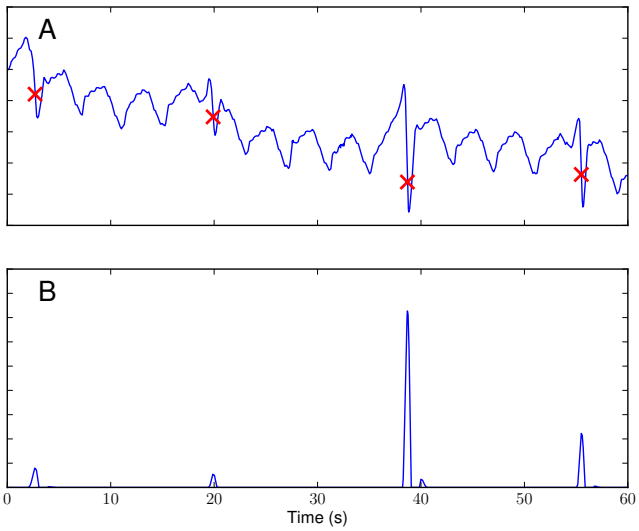

Fig. 1. A gastric slow wave signal (A) and the corresponding detection signal S_t (B). Note that S_t is zero or very close to zero a large proportion of the time, and the spikes in (B) correspond to the slow wave events in (A).

(Fig. 1), and in such cases the threshold was very close to the signal mean multiplied by the same scalar parameter. If the majority of the signal values in the window were zero the median absolute deviation (3) was equal to the signal mean, and if more than half were close to or equal to zero then the median absolute deviation was very close to the signal mean. Calculating a moving mean of the signal was much less computationally intensive than the median absolute deviation defined above and this was used instead.

4) Marking Events: As prescribed by the FEVT method [6], times at which the detection signal exceeded the threshold were classed as potential slow wave events. The method used in this online system differs from that described as part of the FEVT algorithm in the way in which slow wave events were identified from these potential points.

The method used online similarly defines a set of potential times based on the detection signal F and threshold T (4).

$$u = \{t \mid F(t) \geq T(t)\} \tag{4}$$

Differing from the FEVT method, slow wave events were identified from these potential times using a time window of half width t_{lim}. The elements of u that have the greatest magnitude detection signal $F(t)$ of any other element in u within the time threshold were identified as the exact time of a slow wave.

This half width was a tunable parameter but its purpose was to prevent multiple slow waves being identified within too close a time period, as typically several points during a slow wave are identified as potential slow wave events. To select just one, this parameter should be at least as long as the expected length of a slow wave event (for example 2 seconds) and at most as long as the time between subsequent slow wave events (for example 10 seconds for slow waves at 6 cycles per minute).

B. Channels with high false positive (FP) rates

There are situations in which a section from a recording can have a high false positive rate but few true positives and few false negatives. Automatically identifying these bad channels is desirable as they can be indicative of a poor electrical connection or a loss of contact with the serosa. If a single channel were classified as being bad it may be difficult or unnecessary to address the problem, but if a large section of the electrode array consists of bad channels then knowing this when the experiment is taking place gives the operators the opportunity to check the connections or adjust the array for better contact.

A moving estimate of the kurtosis $k(V)$ of a window from a signal V, defined in (5), was trialled and was observed to correctly identify many bad channels while rarely classifying a good channel as bad. The kurtosis was calculated after the signals had been filtered to remove noise and also after the baseline wander had been removed. In good channels, the signal voltage generally had a small range, with occasional large perturbations corresponding to slow wave events. In contrast, many bad channels had a consistent variation about some mean value, especially those that had high components of random noise or those that were just picking up a sinusoidal ventilator signal.

$$k(V) = \frac{|V| \sum_{v \in V} (v - \text{mean}(V))^4}{(\sum_{v \in V} (v - \text{mean}(V))^2)^2} - 3 \qquad (5)$$

The kurtosis was calculated for a set of samples for each channel for a sliding window of sufficient length to contain several slow wave events (if such events were present). A kurtosis threshold and time parameter were defined, and the status of a channel was changed (from bad to good or good to bad) when the kurtosis was less than (to be classified as bad) or greater than (to be classified as good) the threshold for a period of time greater than this time parameter. In practice these thresholds can be set in such a way that most (but not all) bad channels are detected, while rarely incorrectly marking good channels as bad. A kurtosis threshold of 0 and a time parameter of 4 seconds were found to be most effective at classifying bad channels.

C. Graphical Display

The user is presented with a plot that can show either the electrode traces from a single row or single column from the array. Channels on this are marked as either good or bad as their classification changes. The user can rapidly change which row or column is being viewed, so if desired could check each channel by viewing every row or column.

The user is also presented with two-dimensional animated maps, with cells corresponding to the electrodes, and these are able to show a range of information. A map shows wave events as they are detected, which allows the user to see slow waves move through the array. The map also shows good and bad channels as their classifications change. The user is also able to see information such as the detection signal magnitude, the amplitude of wave events, the current moving kurtosis value and several other types of information. Some of these data, such as the current kurtosis value, give a more responsive representation of what is occurring, but are often more subjective to interpret than for example the wave event animations or bad channel classification. It is possible to overlay such animations, though only some combinations (such as wave events and good/bad classification) can be meaningfully interpreted.

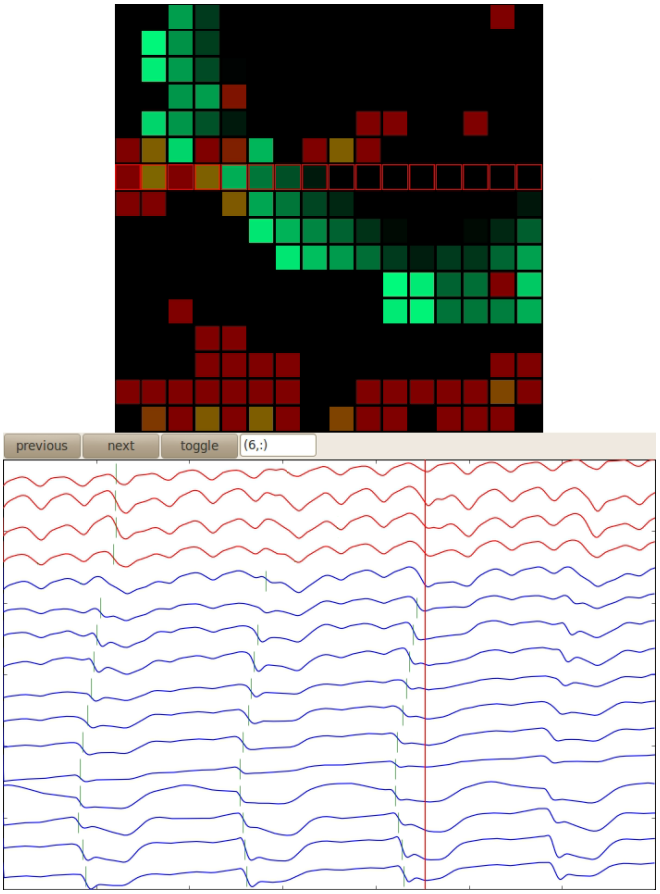

Fig. 2. An example of a user interface configuration showing an activation animation (top) and a 60 second trace of the top row of electrodes (bottom). The red bar in the trace indicates the time of the data in the animation, and the green vertical lines indicate detected slow waves. Red electrodes at the top indicate bad channels, and the green indicates the time since the last activation. Bright green indicates a current activation and black indicates no activation in more than 2 seconds.

III. Results

An online slow wave detecting system was built, and a user interface created (Fig. 2) that conveys information to the user as a study is being performed.

A. Delay

The slow wave detection system is non-causal, in that determining whether or not a slow wave occurs at time t requires knowledge of the input signal at time $t + d$. Practically, this means that when a signal at time t is recorded it becomes possible to determine whether or not there was a slow wave event at time $t-d$, where d is the delay inherent to

the detection system. For offline analysis this is not important but in an online setting it can be significant.

1) Wave Event Delay: The calculation of the NEO (1) requires knowledge of the next input value, so at 32 Hz this induces a delay of $1/32$ seconds. However this is then smoothed with a centred moving average filter which induces a further delay of 0.5 seconds.

Of greater significance, the threshold requires the future 15 seconds of detection signals and this is the source of the majority of the delay in the system. The other source of significant delay is the final marking of events described in Section II-A.4 which requires all of the potential slow wave events in the future 3 seconds to decide whether to accept or reject a current potential slow wave as a true slow wave.

2) Bad Channels Delay: The delay associated with the detection of bad channels is more difficult to quantify. The measure that is used uses a moving estimate of the kurtosis in large window and the delay for a channel to change is at most the length of this window. However, in practice the status tends to change earlier. As slow waves enter a window that previously contained no slow waves the kurtosis rises immediately, and the classification can change after only a short delay.

B. Validation

1) Detection Method: Tests were performed using data acquired from a porcine gastric slow wave mapping study [8]. Though the methods for detection were created for use in an online system, they can also be used directly on a prerecorded file. Instead of producing output in the form of a visualization the output of the analysis can be saved to file. Using this method, prerecorded data were analysed with this system and the output was compared to analysis done by hand and with existing offline techniques. As the method used was very similar to the FEVT algorithm, results were found to be very similar.

2) Online acquisition and display: When used online, the detection methods use streamed data from a network socket. These data were the same as the data that the recording software saves to file. A test program was written that reads data from prerecorded files and streams that data to a socket in the same way that the recording software does, emulating its operation. Tests could then be performed with a system that acted in the same way as the recording software and system (as it would act when recording data), requiring no hardware but rather software and data files. The data acquisition system, detection system and display were tested in this way with prerecorded data from porcine gastric slow wave studies.

C. Accuracy

When used for offline analysis the FEVT method has a positive predictive value of 0.93 and sensitivity of 0.94-0.96 [6]. In channels where slow waves were present the results for the online system are similar (in an eight channel 400 second recording the positive predictive value was 0.92 and the sensitivity was 0.95). The most common cause of false positives were situations where there was a large gap between subsequent slow waves. The threshold became low in this situation and sudden drops in signal voltage were incorrectly identified as slow waves.

In channels with no slow waves it was found that many false positives are detected. The presence of any uncommon slow wave-like change in voltage was detected, as the criteria for slow wave identification relies on there being true slow waves present for comparison. If there are none, the methods perform poorly and for that reason detection of such bad channels is important, and the bad channel detection method is able to to correctly identify many channels of this sort. For analysis offline that is less important as such channels can be removed by hand.

IV. Discussion

This work presents a new framework for the online analysis of multi-electrode GI slow wave recordings. Analysing these signals online will complement the offline analysis and provide experimental benefits. Detecting poor quality recordings early or detecting opportunities to better target areas of interest will improve experimental outcomes. Because the system provides accurate spatio-temporal detail with only modest lag new experiments may be possible where experimental protocols change in response to dynamic changes in electrical activity.

References

[1] G. O'Grady, P. Du, L. K. Cheng, J. U. Egbuji, W. J. E. P. Lammers, J. A. Windsor, and A. J. Pullan, "Origin and propagation of human gastric slow-wave activity defined by high-resolution mapping," *Am. J. of Physiol. Gastrointest. Liver Physiol.*, vol. 299, no. 3, pp. G585–G592, 2010.

[2] W. J. E. P. Lammers, L. Ver Donck, B. Stephen, D. Smets, and J. A. J. Schuurkes, "Focal activities and re-entrant propagations as mechanisms of gastric tachyarrhythmias," *Gastroenterology*, vol. 135, no. 5, pp. 1601–1611, 2008.

[3] L. Ver Donck, W. J. E. P. Lammers, B. Moreaux, D. Smets, J. Voeten, J. Vekemans, J. A. J. Schuurkes, and B. Coulie, "Mapping slow waves and spikes in chronically instrumented conscious dogs: implantation techniques and recordings," *Med. Biol. Eng. and Comput.*, vol. 44, no. 3, pp. 170–178, 2006.

[4] P. Du, G. O'Grady, J. U. Egbuji, W. J. Lammers, D. Budgett, P. Nielsen, J. A. Windsor, A. J. Pullan, and L. K. Cheng, "High-resolution mapping of in vivo gastrointestinal slow wave activity using flexible printed circuit board electrodes: methodology and validation," *Ann. Biomed. Eng.*, vol. 37, no. 4, pp. 839–846, 2009.

[5] C. Cabo and D. S. Rosenbaum, Eds., *Quantitative Cardiac Electrophysiology*. Marcel Dekker, 2002, pp. 403–409.

[6] J. C. Erickson, G. O'Grady, P. Du, C. Obioha, W. Qiao, W. O. Richards, L. A. Bradshaw, A. J. Pullan, and L. K. Cheng, "Falling-Edge, Variable Threshold (FEVT) Method for the Automated Detection of Gastric Slow Wave Events in High-Resolution Serosal Electrode Recordings," *Ann. Biomed. Eng.*, vol. 38, no. 4, pp. 1511–1529, 2010.

[7] J. Kaiser, "Some useful properties of Teager's energy operators," in *Proceedings of the IEEE International Conference on Acoustic Speech and Signal Processing*. IEEE, 1993, pp. 149–152.

[8] J. U. Egbuji, G. O'Grady, P. Du, L. K. Cheng, W. Lammers, J. A. Windsor, and A. J. Pullan, "Origin, propagation and regional characteristics of porcine gastric slow wave activity determined by high-resolution mapping," *Neurogastroent. & Motil.*, vol. 22, no. 10, pp. e292–e300, 2010.